ELSEVIER

Nuclear Physics A 596 (1996) 187-198

NUCLEAR PHYSICS A

$2\nu\beta\beta$ matrix elements and the competition between spin-flip and non-spin-flip channels in realistic calculations ★

M. Aunola, O. Civitarese [1], J. Kauhanen, J. Suhonen

Department of Physics, University of Jyväskylä, P.O. Box 35, FIN-40351 Jyväskylä, Finland

Received 24 August 1995

Abstract

Nuclear matrix elements for the two-neutrino double beta decay ($2\nu\beta\beta$) ground-state transitions of ^{76}Ge and ^{130}Te are analyzed in relation with spin-flip and non-spin-flip degrees of freedom. The calculations have been performed using realistic interactions in the framework of the quasiparticle random-phase approximation. Present results confirm the findings of schematic models concerning the competition between these degrees of freedom.

1. Introduction

The nuclear matrix elements of the two-neutrino double beta decay ($2\nu\beta\beta$) have been computed using different models as well as different nuclear-structure scenarios. The current experimental and theoretical status has been summarized in Refs. [1,2]. The most challenging question concerning the $2\nu\beta\beta$ decay rate is the suppression of the involved nuclear double Gamow–Teller (DGT) matrix element, as inferred from data. Several attempts to explain this behaviour have been reported during the last years since the pioneering works of Primakoff and Rosen [3] and Haxton and Stephenson [4]. For a detailed review of the theoretical aspects the reader is referred to Ref. [5].

Recently the suppression mechanism of the $2\nu\beta\beta$ ground state to ground state (g.s.) transition has been reanalyzed, using schematic models [6,7]. The cancellation of the

★ Supported by the Academy of Finland, contract no. 2856.

[1] Dept. of Physics. Univ. of La Plata, C.C.67 (1900) La Plata, Argentina. Fellow of the CONICET.

SSDI 0375-9474(95)00407-6

associated nuclear matrix element, due to the competition between the spin-flip and non-spin-flip contributions, has been studied in Ref. [7]. As stated in Ref. [7], the strongly destructive interference between non-spin-flip and spin-flip transitions may be responsible for the almost complete suppression of the DGT matrix elements. Also it has been shown that this effect is present even when particle–particle interactions are turned off.

Since the studies of Ref. [7] have been done in a schematic model it is important to confirm these results in a realistic situation. This is the main aim of this article. In particular, we want to extract information about the possible existence of some symmetry underlying the mechanism found in Ref. [7].

For the present work we have chosen realistic two-body matrix elements extracted from the Bonn potential and used them to compute nuclear wave functions and beta-decay amplitudes. The basic elements of the formalism are briefly reviewed in Section 2. A more detailed presentation can be found in Ref. [8]. In Section 3 the $2\nu\beta\beta$ g.s. transitions ^{76}Ge $\rightarrow$ ^{76}Se and ^{130}Te $\rightarrow$ ^{130}Xe are analyzed. The results are discussed in terms of spin-flip and non-spin-flip contributions and they are compared with previously obtained results of the schematic model of Ref. [7]. Finally, the conclusions are drawn in Section 4.

2. Formalism

The procedure to calculate the DGT matrix element within the proton–neutron QRPA (pn-QPRA) approach is a standard one. It consists in evaluating the expression [8]

$$M_{\mathrm{DGT}} = \sum_m \frac{\beta_m^+ \beta_m^-}{(\frac{1}{2}Q_{\beta\beta} + E_m - M_i)/m_e + 1} \tag{1}$$

by introducing the full set of virtual 1^+ excitations, with energies E_m, of the intermediate double-odd nucleus and the associated Gamow–Teller single-beta transition densities

$$\beta_m^- = (1_m^+ || \hat{\beta}^- || 0_i^+) \tag{2}$$

and

$$\beta_m^+ = \sum_{m'} (0_f^+ || \hat{\beta}^- || 1_{m'}^+) \langle 1_{m'}^+ | 1_m^+ \rangle . \tag{3}$$

The quantity $\langle 1_{m'}^+ | 1_m^+ \rangle$ is the overlap of the two different pn-QPRA representations for the set of 1^+ states [8]. The single beta-decay operator $\hat{\beta}^-$, in its quasiparticle representation, is given by

$$\begin{aligned} \hat{\beta}_{1M}^- = \sum_{pn} \sigma(pn) [& u_p v_n A^\dagger(pn, 1M) + v_p u_n A(pn, 1\bar{M}) \\ & - u_p u_n B^\dagger(pn, 1M) + v_p v_n B(pn, 1\bar{M})], \end{aligned} \tag{4}$$

where u and v are the BCS occupation amplitudes, $\sigma(pn)$ is a reduced matrix element of the Pauli spin operator between a proton (p) and a neutron (n) single-particle state. The operators $A^\dagger(pn, 1M)$ and $B^\dagger(pn, 1M)$ are quasiparticle pair operators which create a pn pair coupled to angular momentum 1 with projection M, or scatter a neutron into a proton with the same coupling, respectively. A similar expression holds for the $\hat{\beta}^+$ operator.

The reduced matrix elements of Eqs. (2) and (3) can be written in the pn-QPRA representation [8] starting from the phonon creation operator

$$\Gamma^\dagger_{1M}(m) = \sum_{pn} \left[X_{pn}(1^+m) A^\dagger(pn, 1M) - Y_{pn}(1^+m) A(pn, 1\bar{M}) \right]. \tag{5}$$

The forward- and backward-going amplitudes X and Y are obtained from the diagonalization of the two-body interaction in the pn two-quasiparticle basis. The QRPA matrix equations involved can be found in textbooks [9] and the specific form needed in the present application can be found in Ref. [10].

Following the procedure of Ref. [8] the matrix elements of the two-body interaction in the pn channel are renormalized by the particle–hole and particle–particle strength factors $g_{\rm ph}$ and $g_{\rm pp}$. The value of $g_{\rm ph}$ is determined by the empirical position [11] of the Gamow–Teller giant resonance (GTGR) in the odd–odd intermediate nucleus. The physical values of $g_{\rm pp}$ are known [5,12] to be near unity. However, the precise value of the $g_{\rm pp}$ parameter is not given by the pn-QPRA method [5], but additional information, e.g. extracted from the single beta decay, can be used to define the physically acceptable range of values for this parameter [13].

To summarize, we have taken the G-matrix elements of the Bonn potential and constructed the effective two-body matrix elements as described above, including pairing correlations and renormalizing the particle–particle and the particle-hole channels of the proton–neutron interaction separately in the pn-QPRA method. With the corresponding set of solutions for E_m, $X(1^+m)$ and $Y(1^+m)$, which are the energies and the amplitudes of the 1^+ states, we have computed the DGT matrix element of Eq. (1). As discussed in Ref. [7], the pn-QPRA contributions to the matrix element of $\hat{\beta}^-$ of Eq. (4) (and the corresponding ones for $\hat{\beta}^+$) can be split into "spin-flip" ($j_p = j_n \pm 1$) and "non-spin-flip" ($j_p = j_n$) contributions defined by

$$\beta^-_m(\text{spin-flip}) = \sum_{j_p = j_n \pm 1} \sigma(pn) \left[u_p v_n X_{pn}(1^+m) + v_p u_n Y_{pn}(1^+m) \right], \tag{6}$$

$$\beta^-_m(\text{non-spin-flip}) = \sum_{j_p = j_n} \sigma(pn) \left[u_p v_n X_{pn}(1^+m) + v_p u_n Y_{pn}(1^+m) \right], \tag{7}$$

respectively, yielding for the DGT matrix element (1) the contributions that will be denoted as $M_{\rm DGT}$(spin-flip), $M_{\rm DGT}$(non-spin-flip) and $M_{\rm DGT}$(interference), in a self-explanatory notation.

In the next section we shall illustrate the above splitting in the cases of ^{76}Ge and ^{130}Te g.s. $2\nu\beta\beta$ decays.

3. Results and discussion

As stated in the introduction, we shall see whether the predictions of the schematic model of Ref. [7] about the competition between the spin-flip and the non-spin-flip transitions are confirmed by the present realistic calculations. With this aim, we have proceeded by setting all the elements needed in the calculation as follows:

(i) The single-particle basis: we have performed the calculations using two sets of single-particle energies, the ones coming from the Woods–Saxon potential [14] (WS) and the ones adjusted to the observed sequence of levels near the fermi surface. In the following, this modified single-particle basis will be called the adjusted Woods–Saxon (AWS) basis.

(ii) Pairing effects: we have adjusted pairing strengths to reproduce the observed odd-even mass differences. The renormalization of the matrix elements, coming from the G-matrix of the Bonn potential, has been studied in the WS and AWS basis.

(iii) The parameters of the proton–neutron channels of the G-matrix interaction: we have searched for the optimal values of the particle–hole strength ($g_{\rm ph}$) and the particle–particle strength ($g_{\rm pp}$) by reproducing the energy systematics of the Gamow–Teller giant resonance (GTGR) and by calculating the single-beta decay feeding of the initial and final nuclei ^{76}Ge (from ^{76}Ga), ^{76}Se (from ^{76}Br and ^{76}As), ^{130}Te (from ^{130}Sb) and ^{130}Xe (from ^{130}I and ^{130}Cs).

(iv) The decomposition of the DGT matrix element: we have computed the matrix element (1) for g.s. transitions and analyzed the contribution of the spin-flip and non-spin-flip modes (hereafter denoted as $\mu = 1$ and 0, respectively) to it, as done in Ref. [7].

3.1. The single-particle basis

In the case of $A = 76$ we have adopted for the valence space, both for protons and neutrons, the p-f and s-d-g shells, complemented with the $h_{11/2}$ intruder orbital. For $A = 130$ we use the s-d-g and p-f-h shells and the $i_{13/2}$ intruder state. The WS potential is parametrized as in Ref. [14]. It gives approximately the correct sequence of single-particle energies. One exception is the position of the intruder states, i.e. $g_{9/2}$ for neutrons and protons in the p-f shell and $h_{11/2}$ for the s-d-g shell. We have shifted the position of the intruder states and found that these rearrangements led to better results for the quasiparticle energy spectra. At the same time some other small adjustments in the WS energies were made. A characteristic feature of this AWS spectrum is that it yields a higher density of levels, near the Fermi surface, as compared to the WS results.

3.2. Pairing effects

To test the quality of the chosen single-particle basis we have performed calculations of odd–even mass differences, pairing occupations and gaps both for the WS and AWS bases. The pairing strengths for the AWS basis are slightly smaller, by at most 10%,

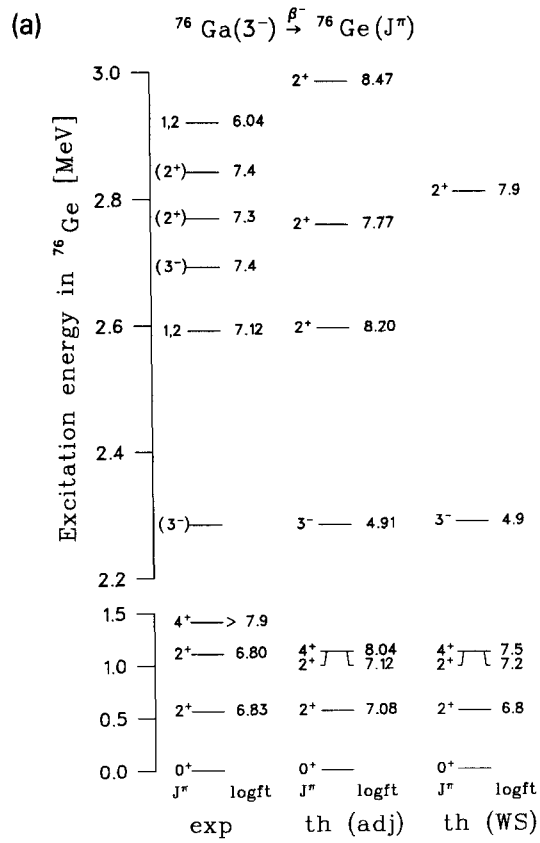

Fig. 1. Systematics of energy levels and $\log ft$ values for single β^- and β^+ transitions leading to $A = 76$ and 130. These transitions feed the initial and final nuclei participating in the double beta decays of ^{76}Ge and ^{130}Te. The theoretical values (th) obtained by diagonalizing the proton–neutron and proton–proton and neutron–neutron interactions, in the Woods–Saxon (WS) and the modified Woods–Saxon (adj) basis, are compared with the corresponding experimental (exp) values.

than the ones for the WS basis. Because of this renormalization, which is affecting the proton states more than the neutron ones, the AWS quasiparticle spectra are, in general, more realistic than the WS ones. The difference between the WS and AWS quasiparticle states are more significant for the $A = 76$ system than for the $A = 130$ system. Due to the shifting of the intruder state and the slight compression of the AWS major shell, the corresponding quasiparticle spectrum is narrow as compared with the WS one.

3.3. *The parameters of the proton–neutron channels of the G-matrix interaction*

To assess the quality of the two-body matrix elements we have performed a systematics of the energy levels and beta-decay feeding patterns for nuclei in the neighbourhood of the double beta decay systems of $A = 76$ and 130. We have analyzed the following allowed and forbidden single β^- and β^+ decays: ^{76}Ga$(3^-) \rightarrow {}^{76}Ge(J^\pi)$, ^{76}As$(2^-)$

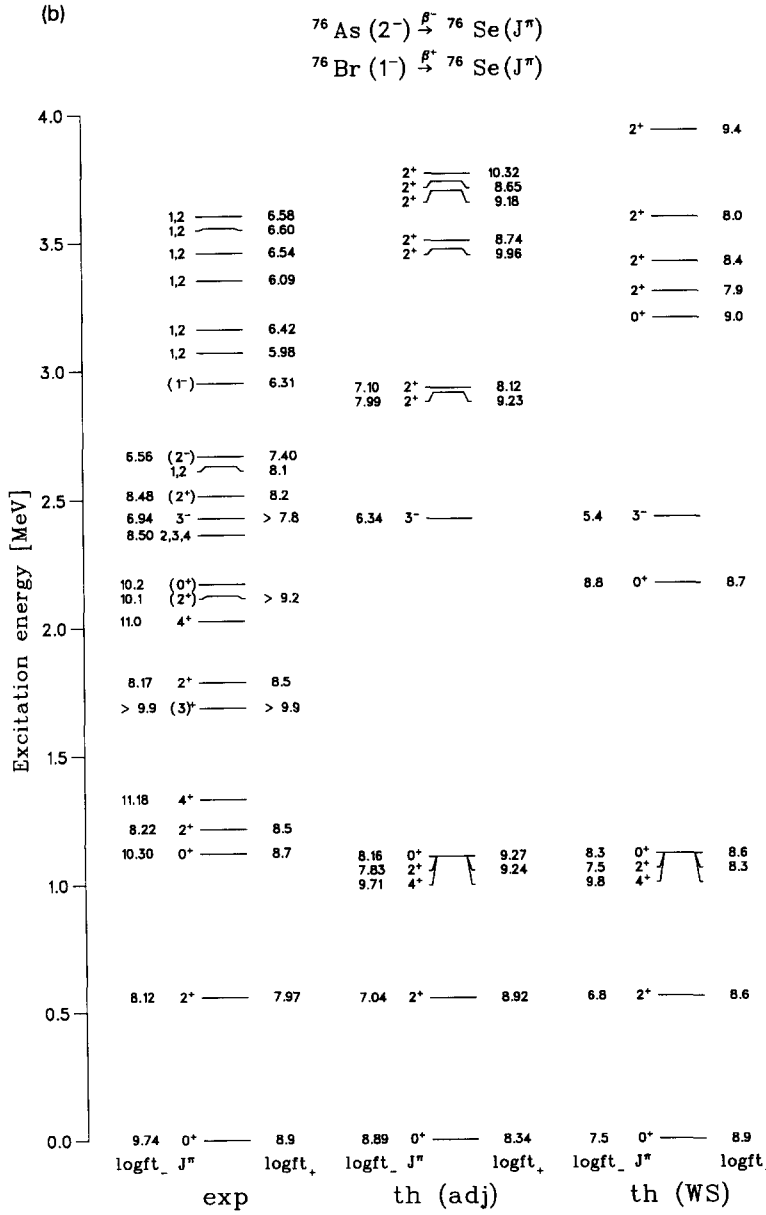

Fig. 1 — continued.

$\rightarrow {}^{76}\mathrm{Se}(J^{\pi})$, ${}^{76}\mathrm{Br}(1^{-}) \rightarrow {}^{76}\mathrm{Se}(J^{\pi})$, ${}^{130}\mathrm{Sb}(5^{+}) \rightarrow {}^{130}\mathrm{Te}(J^{\pi})$, ${}^{130}\mathrm{I}(2^{+}) \rightarrow {}^{130}\mathrm{Xe}(J^{\pi})$, ${}^{130}\mathrm{Cs}(1^{+}) \rightarrow {}^{130}\mathrm{Xe}(J^{\pi})$. The corresponding results are shown in Fig. 1. In general, the agreement between experiment and the theory, concerning the energies and the log ft values, is fairly good both for the WS and AWS basis. In particular, one can reproduce the log ft values of transitions to the 2_1^+ and the two-phonon 0^+, 2^+ and 4^+ states, both for allowed and forbidden decays.

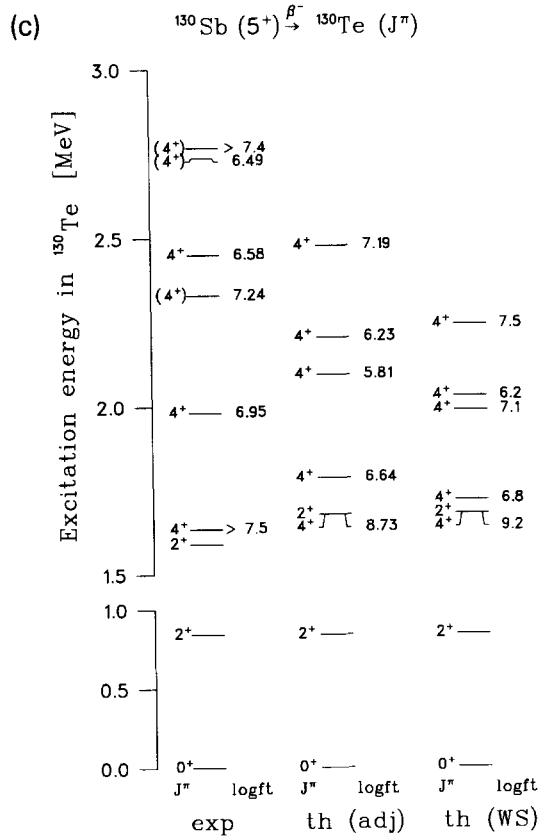

Fig. 1 —continued.

3.4. The decomposition of the DGT matrix element

Concerning the calculation of the DGT matrix element (1), shown in Fig. 2 as a solid line, we have chosen g_{ph} values which reproduce the observed energy of the GTGR state in ^{76}As and ^{130}I. Then we allowed the g_{pp} parameter to vary from 0.0 to the breaking point of the *pn*-QPRA [9]. In the following, we have calculated the spin-flip decomposition for two extreme values of g_{pp}, namely for $g_{pp} = 0.0$ and for a g_{pp} value near the breaking point. For $A = 76$ we discuss the AWS basis and for $A = 130$ the WS basis. For both masses the values $g_{pp} = 0.0$ and 0.7 are chosen.

For the case of ^{76}Ge, in the adopted g_{pp} range, the theoretical $2\nu\beta\beta$ half life varies between 8.4×10^{19} y ($g_{pp} = 0.0$) and 3.0×10^{20} y ($g_{pp} = 0.70$). The value for which the *pn*-QPRA breaks down is at $g_{pp} = 0.8$. As seen in Fig. 2 the values of the DGT matrix element (1) are very similar in both bases, for the above-mentioned g_{pp} range.

For the ^{130}Te the WS and AWS bases produce similar results, both for the single beta and double beta decay observables. The theoretical $2\nu\beta\beta$ half life varies between 3.3×10^{18} y ($g_{pp} = 0.0$) and 3.1×10^{20} y ($g_{pp} = 0.70$). The breaking point of the *pn*-QPRA lies at $g_{pp} = 0.71$ for the WS basis and at $g_{pp} = 0.60$ for the AWS basis.

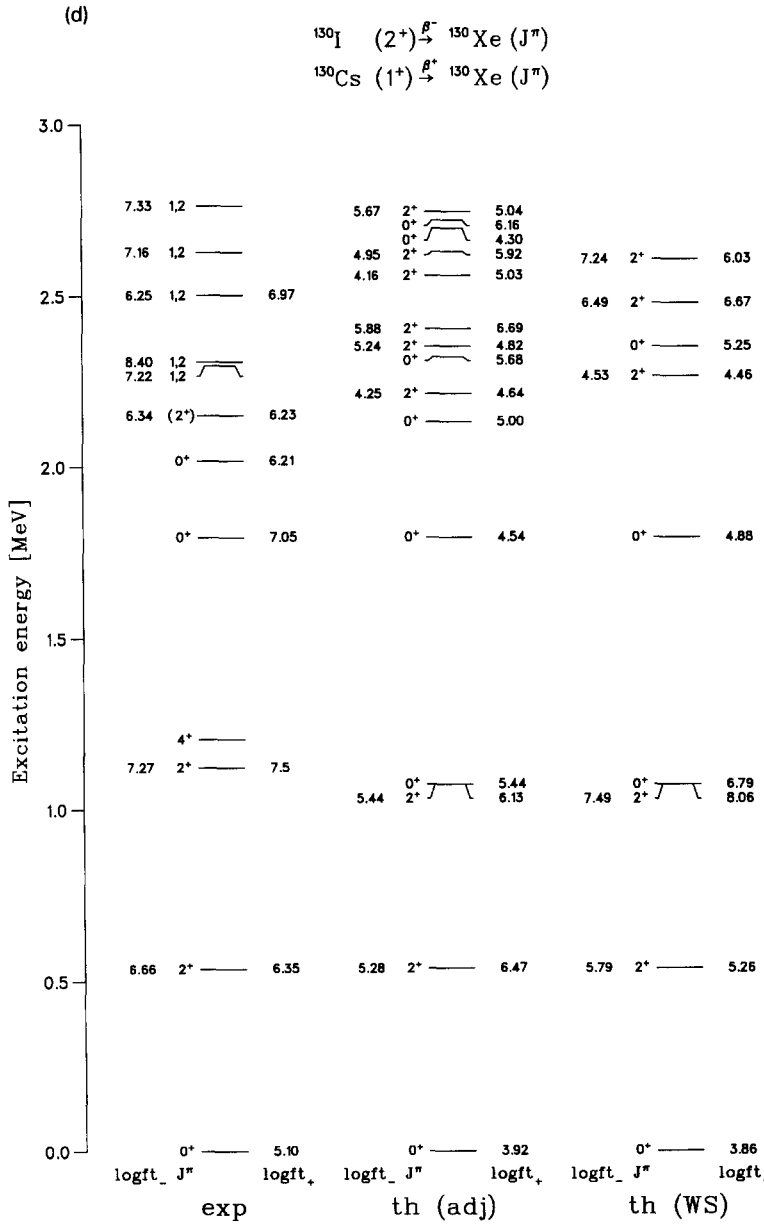

Fig. 1 — continued.

In spite of the fact that some of the above-mentioned features have been already discussed in the literature, we have included them here in order to see if the findings of Ref. [7], concerning the spin-flip decomposition, are valid generally in realistic calculations.

The DGT matrix elements, decomposed into μ = 0,1 and interference terms, for A = 76 and 130, are shown in Fig. 2. The agreement between the predicted general

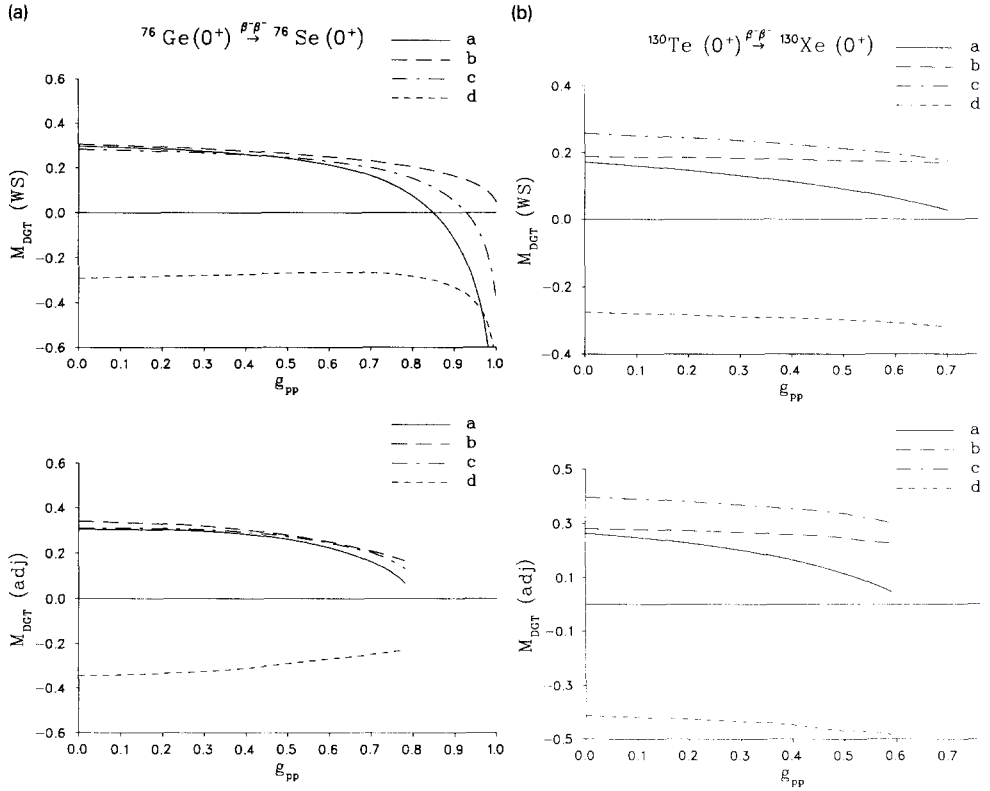

Fig. 2. Total matrix element M_{DGT} of Eq. (1) (case a) and its non-spin-flip (case b), spin-flip (case c) and interference (case d) contributions as functions of the particle–particle strength g_{pp}. (a) The results for $A = 76$ and (b) corresponds to $A = 130$. Results obtained with the Woods–Saxon (WS) basis and with the empirical basis (adj), as discussed in the text, are shown.

trends of the schematic model of Ref. [7] and the present case is remarkable. The results of the realistic calculation show that the suppression of the DGT matrix element is due to the competition between the interference term and the $\mu = 0$ and 1 terms. As seen from this figure, the different terms vary slowly, for increasing values of g_{pp}, except at the breaking point. The difference between the $\mu = 0$ and 1 terms is larger for the $A = 130$ case, and practically negligible for the $A = 76$ case. For both cases the interference term compares with each of the $\mu = 0$ and 1 terms.

The $\mu = 0,1$ and interference contributions to the DGT matrix element, as a function of the *pn*-QPRA energy, are shown in Fig. 3 for the $A = 76$ system and in Fig. 4 for the $A = 130$ system. Again, the results of the realistic calculations resemble the results of the schematic model [7]. For the $A = 76$ case it is seen that with increasing values of g_{pp} the interference term loses its coherence, contrary to the $A = 130$ case. However, as for the schematic model, one sees that the value of the total DGT matrix element is not given by a single *pn*-QPRA intermediate state. The low-lying transitions are mostly of the spin-flip type and they are more affected by the increase of the particle–particle

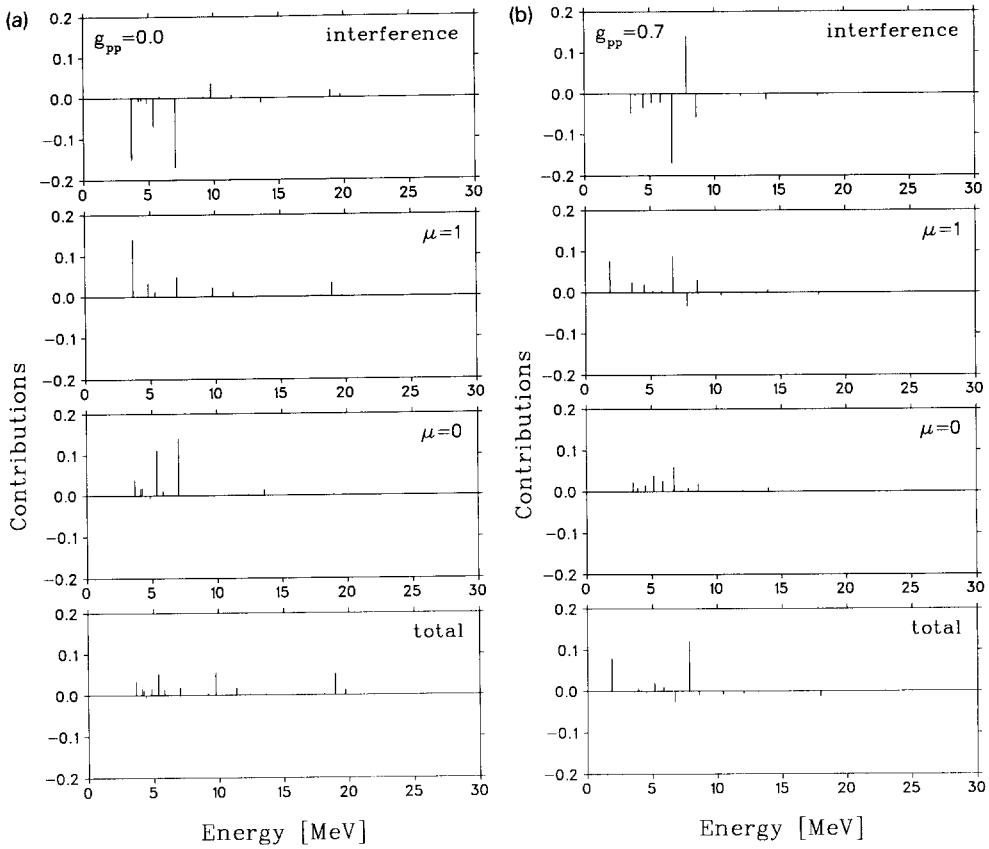

Fig. 3. Contributions to the total DGT matrix element (1), for $A = 76$, as functions of the energy of the intermediate 1^+ states for $g_{pp} = 0.0$ and 0.7. The results correspond to the AWS basis and they show spin-flip ($\mu = 1$), non-spin-flip ($\mu = 0$), interference and total contributions to the DGT matrix elements, as discussed in the text.

correlations. Once again, this coincides with the findings of the schematic model. One has to note that important contributions can arise even from relatively high energies. This is more apparent for the $A = 76$ system, but it is equally important for the $A = 130$ system.

The above analysis shows that the features observed in the context of the schematic model [7] are also present in realistic calculations, both qualitatively and quantitatively.

4. Conclusions

In this work we have studied a mechanism which leads to the strong suppression of the $2\nu\beta\beta$ decay matrix elements. We have studied the behavior of the relevant DGT matrix element in a realistic model. The present results confirm the findings of the schematic model of Ref. [7] concerning the interference between non-spin-flip and

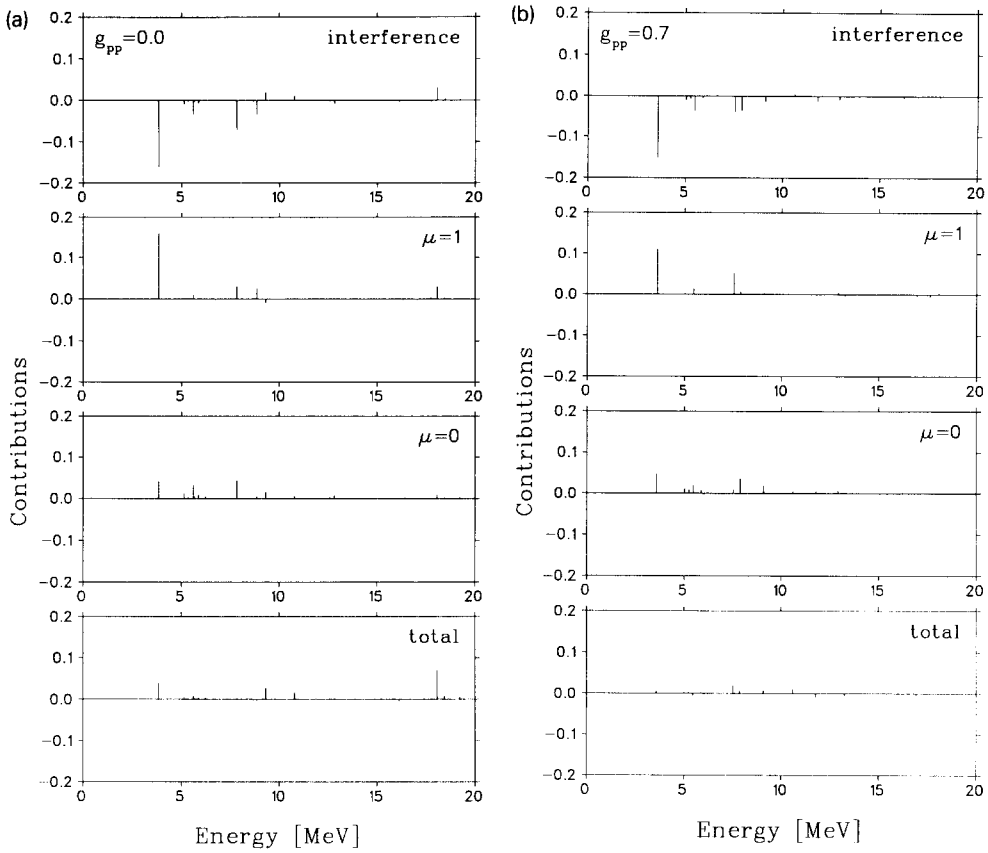

Fig. 4. Contributions to the total DGT matrix element for $A = 130$ as functions of the energy of the intermediate 1^+ states for $g_{pp} = 0.0$ and 0.7 in the WS basis. The quantities are denoted as explained in the caption of Fig. 3.

spin-flip transitions, which is strongly destructive. This interference is found even when the particle–particle interactions are switched off and it becomes larger for increasing values of the interaction strength of the proton–neutron particle–particle channel.

Like in the case of the schematic model, the present results show that no dominant contribution can be expected from a single excited state, like the GTGR, and that the $\mu = 1$ and 0 components of the wave functions of the intermediate states do not influence the total matrix element in the same way. This result could be of significance in dealing with the identification of underlying symmetries, like the splitting of the $\mu = 0$ and ± 1 components of the GTGR discussed in Ref. [6]. The pattern proposed in Ref. [6] does not emerge from the present realistic results and perhaps it is restricted to the particular model used in Ref. [6] to represent the $2\nu\beta\beta$ transitions.

References

[1] V.I. Tretyak and Yu.G. Zdesenko, Tables of double beta decay data, Atomic and Nuclear Data Tables (in press).
[2] M.K. Moe, Int. J. Mod. Phys. E 2 (1993) 507;
M.K. Moe and P. Vogel, Ann. Rev. Nucl. Part. Sci. 44 (1994) 237.
[3] M. Primakoff and S.P. Rosen, Ann. Rev. Nucl. Part. Sci. 31 (1981) 145.
[4] W.C. Haxton and G.J. Stephenson Jr., Prog. Part. Nucl. Phys. 12 (1984) 409.
[5] W.C. Haxton, Nucl. Phys. B (Proc. Suppl.) 31 (1993) 88.
[6] A.A. Raduta, D.S. Delion and A. Faessler, Phys. Rev. C 51 (1995) 3008.
[7] O. Civitarese , J. Suhonen and A. Faessler, Nucl. Phys. A, in press.
[8] O. Civitarese and J. Suhonen, Nucl. Phys. A 578 (1994) 62.
[9] P. Ring and P. Schuck, The nuclear many-body problem (Springer, New York, 1980) chap. 8.
[10] P. Vogel and M. Zirnbauer, Phys. Rev. Lett. 57 (1986) 3148.
[11] D.J. Horen et al., Phys. Lett. B 99 (1981) 383.
[12] A. Staudt, T.T.S. Kuo and H.V. Klapdor-Kleingrothaus, Phys. Lett. B 242 (1990) 17.
[13] J. Suhonen and O. Civitarese, Phys. Rev. C 49 (1994) 3055.
[14] A. Bohr and B.R. Mottelson, Nuclear structure, vol. I (Benjamin, New York, 1969).